Cyclic deformation behaviour of a copper bicrystal with single-slip-oriented component crystals and a perpendicular grain boundary: cyclic stress–strain response and saturation dislocation observation

By Z. F. ZHANG and Z. G. WANG

State Key Laboratory for Fatigue and Fracture of Materials, Institute of Metal Research, Academia Sinica, Shenyang, 110015, PR China

ABSTRACT

The cyclic deformation behaviour of a $[\bar{5}\,9\,13]$-$[\bar{5}\,7\,9]$ copper bicrystal with a grain boundary (GB) approximately perpendicular to the stress axis was investigated under constant-plastic-strain control at room temperature in air. In particular, the bicrystal contains two single-slip-oriented component crystals. The results showed that the cyclic stress–strain curve (CSSC) of the bicrystal exhibited two plateau regions in the axial plastic strain range of 1.8×10^{-4}-1.35×10^{-3} and 2.05×10^{-3}-2.56×10^{-3} respectively. The corresponding plateau axial saturation stresses were about 62–64 MPa and 70–71 MPa. During cyclic deformation, only the primary slip system B4 $(111)[\bar{1}01]$ within the two component crystals was activated including the vicinity of the GB at all the applied strain amplitudes. Meanwhile, it is found that the plastic strains carried by the $[\bar{5}\,9\,13]$ and $[\bar{5}\,7\,9]$ grains are obviously different owing to the difference in their orientations. By means of the electron channelling contrast technique in scanning electron microscopy, the surface dislocation patterns of the bicrystal were observed. The dislocation patterns in the two grains also showed an apparent difference. Based on the experimental results above, the effect of crystal orientation on the CSSC, surface slip patterns and saturation dislocation configurations within two grains was discussed.

§1. INTRODUCTION

By comparing the fatigue behaviours of single crystals and polycrystals; it is suggested that the effects of grain boundaries (GBs) and grains on the polycrystals have not been understood sufficiently (Lukáš and Kunz 1994). In general, the bicrystal, because of its simple composition, can be regarded as an ideal model material to reveal the effects of GBs and crystal orientations on the plastic deformation mechanisms of polycrystals. However, most studies on bicrystals were performed under monotonic loading (Hook and Hirth 1967, Hirth 1972, Chuang and Margolin 1973, Rey and Zaoui 1980), and only very limited work on the cyclic deformation behaviour of bicrystals (Hu and Wang 1997, Peralta and Laird 1997) can be found. In our previous work (Hu and Wang 1997), the cyclic deformation behaviour of a copper bicrystal with a perpendicular GB was investigated under constant plastic-strain control. This bicrystal consists of a single-slip-oriented $[\bar{3}45]$ grain and a double-slip-oriented $[\bar{1}17]$ grain. The results showed that the copper bicrystal exhibited a very high saturation stress and did not display an apparent plateau region in its CSSC. In this paper, a copper bicrystal with a perpendicular GB was also selected, but both of the component grains in the bicrystal are oriented for single slip. The aim of the work is to investigate further the effect of each grain on the cyclic deformation behaviour of the bicrystal.

In recent years, the electron channelling contrast (ECC) technique in scanning electron microscopy (SEM) was successfully applied to observe the dislocation patterns of deformed metals, such as in copper single crystals (Gong *et al.* 1997), nickel single crystals (Schwab *et al.* 1996, 1998, Bretschneider, Holste and Tippelt 1997) and polycrystals (Zauter *et al.* 1992). In comparison with the transmission electron microscopy (TEM) technique, the SEM-ECC technique has many attractive features. With this technique, one can obtain information on dislocation arrangements over a large area and at some special sites, for example in the vicinity of GB, within deformation bands (Gong *et al.* 1997) and at the head of crack. With the help of the SEM-ECC technique, the dislocation patterns of the bicrystal can be observed and compared. Furthermore, the effect of cyclic saturation dislocation patterns on the CSSC of the bicrystal can be revealed.

§2. Experimental procedure

A bicrystal with a size of 150 mm × 50 mm × 10 mm was grown from oxygen-free high-conductivity copper of 99.999% purity by the Bridgman method in a horizontal furnace, and the GB was along the growing direction. The fatigue specimen with a GB plane approximately perpendicular to the stress axis was spark machined from the bicrystal plate, and the gauge size is 16 mm × 6 mm × 3 mm. By the X-ray Laue back-reflection method, the two component crystal orientations of the bicrystal were determined as G1 $[\bar{5}\,9\,13]$ and G2 $[\bar{5}79]$, as shown in figure 1 (*a*). It is clear that both of
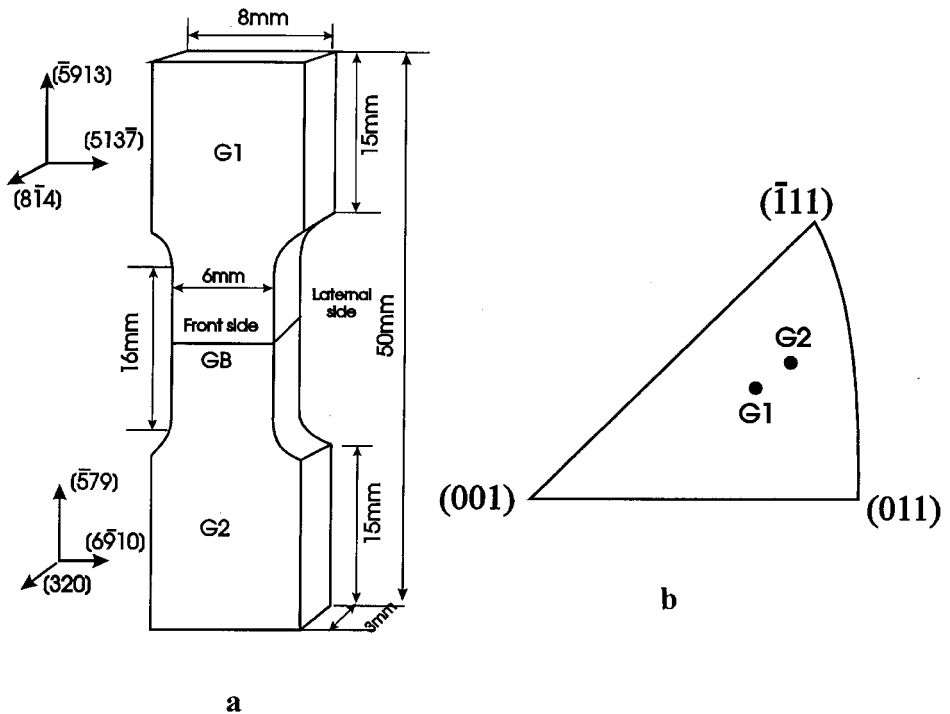

Figure 1.   The crystallographic relations of the $[\bar{5}\,9\,13]$-$[\bar{5}79]$ copper bicrystal; (*a*) crystallographic relations of primary slip with a GB, (*b*) component crystal orientations of the bicrystal.

Table 1. The operation conditions of dislocation pattern observation by the SEM–ECC technique.

Acceleration voltage (kV)	Working distance (mm)	Probe current (nA)	Brightness (%)	Contrast (%)	Scanning rate
20	15–22	2–5	80–90	30–33	TV/2K

the grains are oriented for single slip and show a difference in their orientation. In particular, the Schmid factors of the two grains are quite different and equal to 0.452 (G1) and 0.406 (G2). The crystallographic relations of the two grains in the bicrystal are shown in figure 1(*b*). Before cyclic deformation, all the bicrystal specimens were electropolished carefully for surface observation. Cyclic push–pull tests were performed on a Shimadzu servohydraulic testing machine under constant-plastic-strain control at room temperature in air. A triangular wave with a frequency range of 0.03–0.3 Hz was used. The peak loads in tension and compression were recorded continuously and the hysteresis loops were registered in intervals on an *X*–*Y* recorder until cyclic saturation occurred. The applied axial plastic strain amplitudes $\Delta\varepsilon_{pl}/2$ are in the range 1.8×10^{-4}-2.56×10^{-3}. After cyclic saturation, the bicrystal surfaces were observed to examine slip morphology. Then, those bicrystals were repolished to observe the dislocation patterns within grains and in the vicinity of the GB by the SEM–ECC technique. The operation conditions of SEM-ECC technique are listed in table 1.

§3. Experimental results
3.1. *Cyclic hardening and saturation behaviour*
The cyclic hardening curves at different strain amplitudes are shown in figure 2. Here, the axial stress amplitude is employed. Similar to the results on copper single
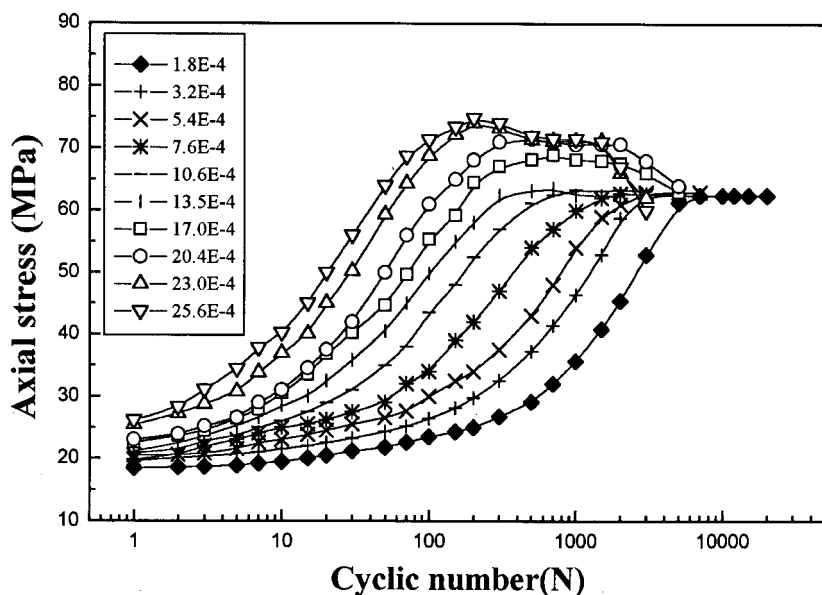

Figure 2. Cyclic hardening curves of the $[\bar{5}\,9\,13]$-$[\bar{5}79]$ copper bicrystal.

Table 2. Cyclic saturation stress and strain data of the copper bicrystal.

$\varepsilon_{pa}(10^{-4})$	σ_{as} (MPa)	τ_{as}^{G1} (MPa)	τ_{as}^{G2} (MPa)
1.8	62.1	28.1	25.3
3.2	62.6	28.3	25.5
5.4	62.7	28.3	25.5
7.6	62.9	28.4	25.6
10.6	63.1	28.5	25.7
13.5	63.7	28.8	25.9
17.0	68.6	31.0	27.9
20.4	70.3	31.8	28.5
23.0	70.6	31.9	28.7
25.6	70.8	32.0	28.9

crystals (Mughrabi 1978), the initial cyclic hardening rates of the bicrystal also increased with increasing plastic strain amplitude. No obvious stress overshooting was observed except at higher strain amplitudes. In comparison with the copper single crystal, the copper bicrystal displayed a relatively shorter saturation region, especially as the strain amplitude was increased owing to the initiation and propagation of fatigue crack along the GB. This phenomenon was also found in the $[\bar{3}45]$-$[\bar{1}17]$ copper bicrystal (Hu and Wang 1997).

The cyclic saturation data of the copper bicrystal are listed in table 2, where the saturation resolved shear stresses $(\tau_{as}^{G1}, \tau_{as}^{G2})$ of the $[\bar{5}\,9\,13]$ and $[\bar{5}79]$ grains are calculated from the axial saturation stresses σ_{as} of the bicrystal by the following equations

$$\tau_{as}^{G1} = \sigma_{as}\Omega_{G1}, \qquad (1)$$

$$\tau_{as}^{G2} = \sigma_{as}\Omega_{G2}. \qquad (2)$$

The CSSC plotted as the axial saturation stress amplitude σ_{as} against the axial plastic strain amplitude ε_{pl} is illustrated in figure 3(a). It is interesting to find that the CSSC of the present bicrystal displays a S shape, which is quite different from the shape found for the $[\bar{3}45]$-$[\bar{1}17]$ copper bicrystal (Hu and Wang 1997) and for the single crystals (Mughrabi 1978, Basinski and Basinski 1992) or the polycrystals (Bhat and Laird 1978; Rasmussen and Pedersen 1980, Lukáš and Kunz 1994). The cyclic saturation axial stress of the present bicrystal first maintained a constant value of 62–64 MPa in the lower axial plastic strain range amplitude of 1.8×10^{-4}-13.5×10^{-4}. With increasing plastic strain amplitude, the cyclic saturation stress increased and approached a constant value of about 70–71 MPa again. This means that the bicrystal with two single-slip-oriented grains displayed two plateau regions in its CSSC. In addition, the plot of the saturation resolved shear stress against the plastic strain is shown in figure 3(b) and will be discussed in the following section.

3.2. Surface slip pattern observation

Surface observation showed that only the primary slip system B4(111)$[\bar{1}01]$ was activated in both $[\bar{5}\,9\,13]$ and $[\bar{5}79]$ grains for all the plastic strain amplitudes applied in this study. The density of slip bands in the $[\bar{5}\,9\,13]$ grain was always higher than that in the $[\bar{5}79]$ grain. As shown in figure 4, the slip patterns in the vicinity of the GB
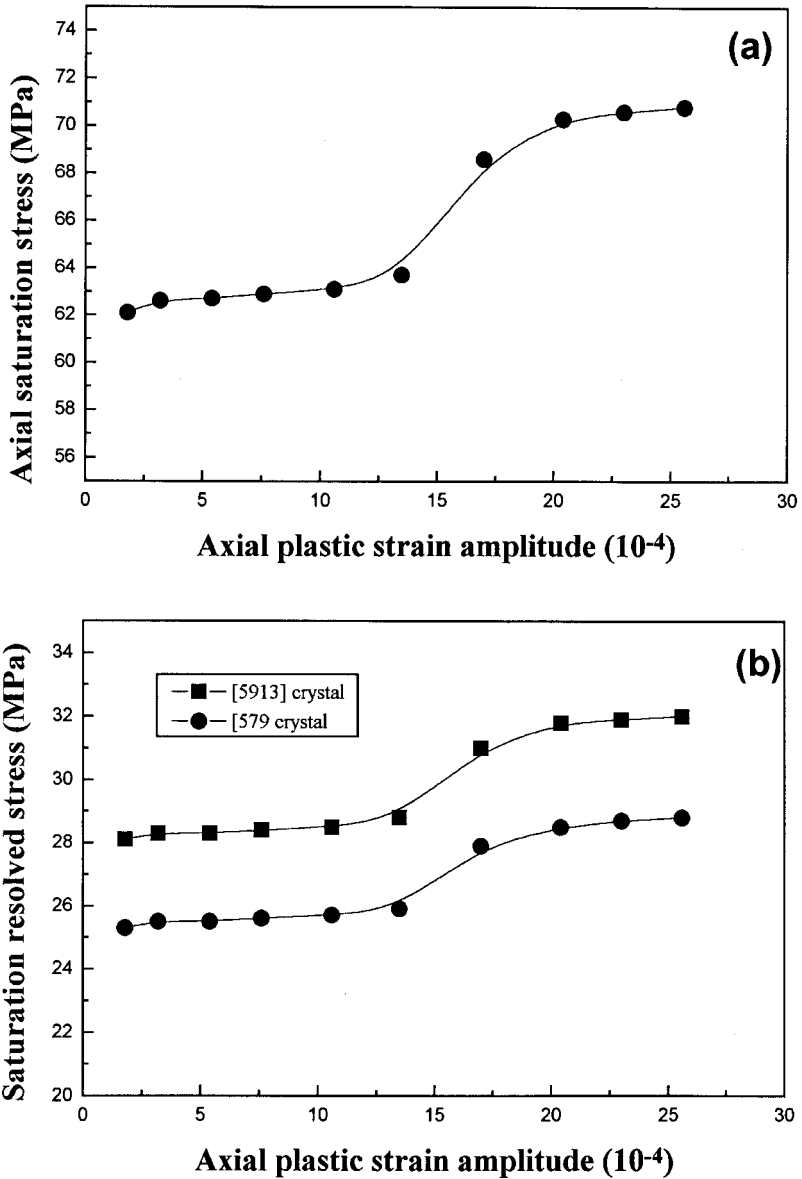
Figure 3. CSSCs of the $[\bar{5}\,9\,13]$-$[\bar{5}79]$ copper bicrystal: (*a*) the curve of axial saturation stress against axial plastic strain; (*b*) the curves of saturation shear stresses of the $[\bar{5}\,9\,13]$ and $[\bar{5}79]$ grains against axial plastic strain.

for the axial plastic strain amplitudes of 3.2×10^{-4} and 1.35×10^{-3} are illustrated. It can be found that no secondary slip occurred including the vicinity of the GB. As the plastic strain amplitude was increased to the range 1.7×10^{-3}-2.56×10^{-3}, deformation bands occurred on the surface of the $[\bar{5}\,9\,13]$ grain, and the slip bands in the $[\bar{5}79]$ grain became denser, as shown in figure 5. Apparently, there is still no evidence of the activation of secondary slip within grains and in the vicinity of the GB, even though the applied plastic strain amplitude was rather high.
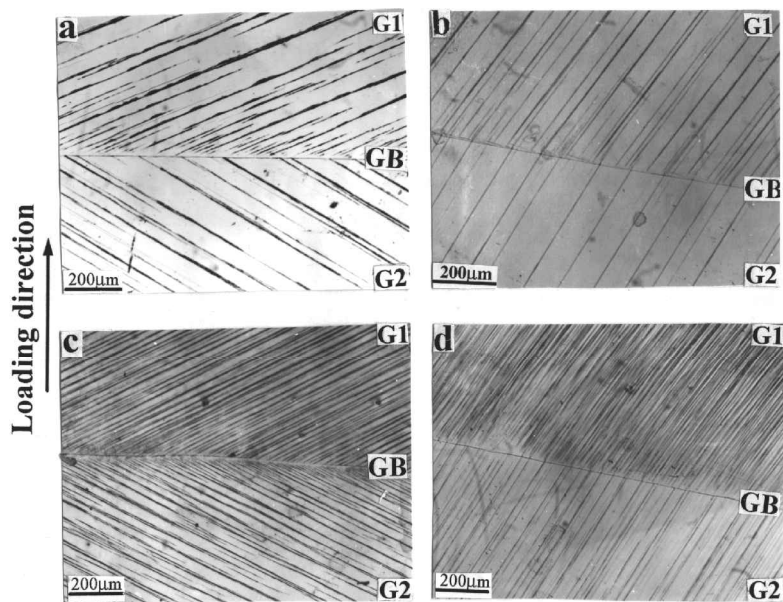
Figure 4. Slip patterns in the vicinity of the GB in the $[\bar{5}\,9\,13]$-$[\bar{5}79]$ copper bicrystal: (a) $\varepsilon_{pl} = 3.2 \times 10^{-4}$ ($N = 10^4$ cycles) (viewed from the front surface); (b) $\varepsilon_{pl} = 3.2 \times 10^{-4}$ ($N = 10^4$ cycles) (viewed from the lateral surface); (c) $\varepsilon_{pl} = 1.35 \times 10^{-3}$ ($N = 5 \times 10^3$ cycles) (viewed from the front surface); (d) $\varepsilon_{pl} = 1.35 \times 10^{-3}$ ($N = 5 \times 10^3$ cycles) (viewed from the lateral surface).
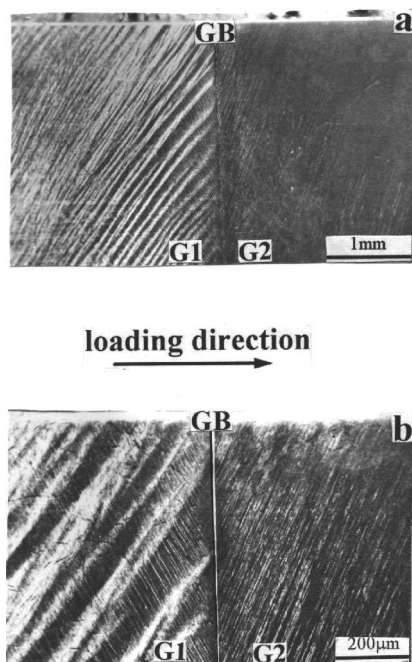

Figure 5. Slip patterns and deformation bands in the $[\bar{5}\,9\,13]$-$[\bar{5}79]$ copper bicrystal cyclically deformed at the plastic strain amplitude of 2.3×10^{-3} for 4000 cycles; (a) at a low magnification; (b) at a high magnification.

In general, it was pointed out that macroscopic compatibility conditions at a GB plane are fulfilled if the total number of independent operating slip systems in both neighbouring crystals for a bicrystal with a parallax GB is four (Kock 1964). The region in the vicinity of a GB often exhibits stress–strain incompatibility and a GB-affected zone was introduced (Rey and Zaoui 1980). However, in the bicrystal with a perpendicular GB, no suitable method was proposed to predict the operation of slip systems. Recently, the studies on the operation of slip systems in the vicinity of a GB in a copper bicrystal with a perpendicular GB (Hu and Wang 1997, Peralta and Laird 1997) showed that multiple slip was activated in the vicinity of the GB. However, as shown in figures 4 and 5, only primary slip can be a observed in the present bicrystal no matter whether at a lower strain amplitude (3.2×10^{-4}) or at a higher strain amplitude (2.56×10^{-3}). This implies that the stress–strain incompatibility at a GB does not always lead to multiple slip.

3.3. *Observations on dislocation patterns*

Instead of the commonly used TEM technique, the SEM–ECC technique was adopted for dislocation pattern observation in the present study. The observations on two crystal surfaces showed that the dislocation patterns became visible in the magnification range 1500–3000. At relatively lower strain amplitudes $(\varepsilon_{pl} = 1.8 \times 10^{-4}\text{-}1.35 \times 10^{-3})$, the saturation dislocation patterns consisted of the typical two-phase structures (Winter 1974, Finney and Laird 1975) within the $[\bar{5}\,9\,13]$ grain, that is persistent slip bands (PSBs) and vein structures, as shown in figures 6 (*a*) and (*b*). Clearly, with increasing plastic strain amplitude, the volume fraction of
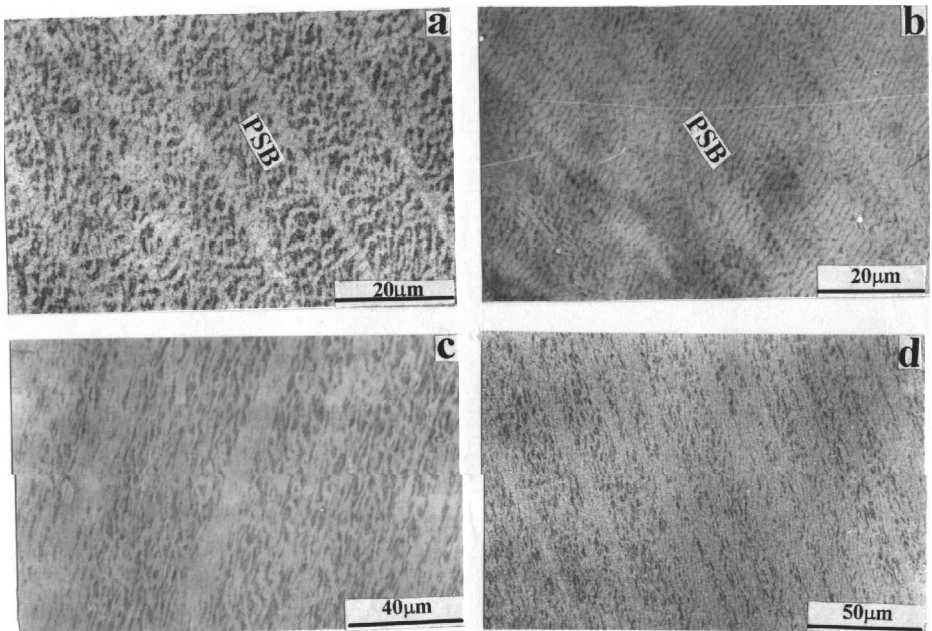

Figure 6. Dislocation patterns within the $[\bar{5}\,9\,13]$ grain: (*a*) $\varepsilon_{pl} = 7.6 \times 10^{-4}$ ($N = 10^4$ cycles); (*b*) $\varepsilon_{pl} = 1.35 \times 10^{-3}$ ($N = 5 \times 10^3$ cycles) and within the $[\bar{5}\,7\,9]$ grain; (*c*) $\varepsilon_{pl} = 7.6 \times 10^{-4}$ ($N = 10^4$ cycles); (*d*) $\varepsilon_{pl} = 1.35 \times 10^{-3}$ ($N = 5 \times 10^3$ cycles) in the lower plateau region of the bicrystal.
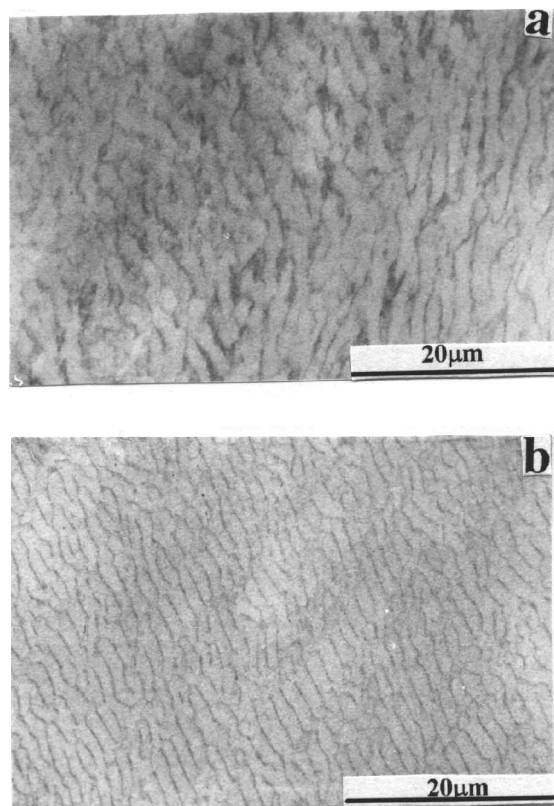
Figure 7.   Dislocation patterns within (a) the $[\bar{5}\,9\,13]$ grain: ($\varepsilon_{pl} = 2.3 \times 10^{-3}$ ($N = 4 \times 10^3$ cycles)) and (b) the $[\bar{5}79]$ grain ($\varepsilon_{pl} = 2.3 \times 10^{-3}$ ($N = 4 \times 10^3$ cycles)) in the upper plateau region.

the PSBs increased. These saturation dislocation patterns in the $[\bar{5}\,9\,13]$ grain were similar to those observed in the single-slip oriented copper single crystal cycled in region B of the CSSC (Laird *et al*. 1986). However, as shown in figure 6(c), the dislocation patterns in the $[\bar{5}79]$ grain cycled at the lower plastic strain amplitude are similar to the loop patches or veins. With increasing plastic strain amplitude, the dislocation patterns in the $[\bar{5}79]$ grain with some parallel wall structures, which are somewhat similar to the PSB, can be observed, but no regular ladder-like dislocation walls can be clearly seen.

At higher strain amplitudes ($\varepsilon_{pl} = 1.7 \times 10^{-3}$-$2.56 \times 10^{-3}$), the dislocation patterns within the $[\bar{5}\,9\,13]$ grain developed into irregular cell structures, as shown in figure 7(a). This dislocation pattern is similar to that observed in region C of the CSSC for copper single crystals. However, as shown in figure 7(b), the dislocation patterns in the $[\bar{5}79]$ grain cycled at the same plastic strain amplitude developed into ladder-like structures and walls, which are typical dislocation arrangements in region B of the CSSC for copper single crystal.

Figure 8 demonstrates the interaction of PSBs in the $[\bar{5}\,9\,13]$ grain with the GB, as revealed by the SEM-ECC technique. It is very interesting to note that the PSB can extend to the GB with a sharp end (figure 8(b)) and produce affected zones in the neighbouring $[\bar{5}79]$ grain, as indicated by the arrows. Those affected zones developed
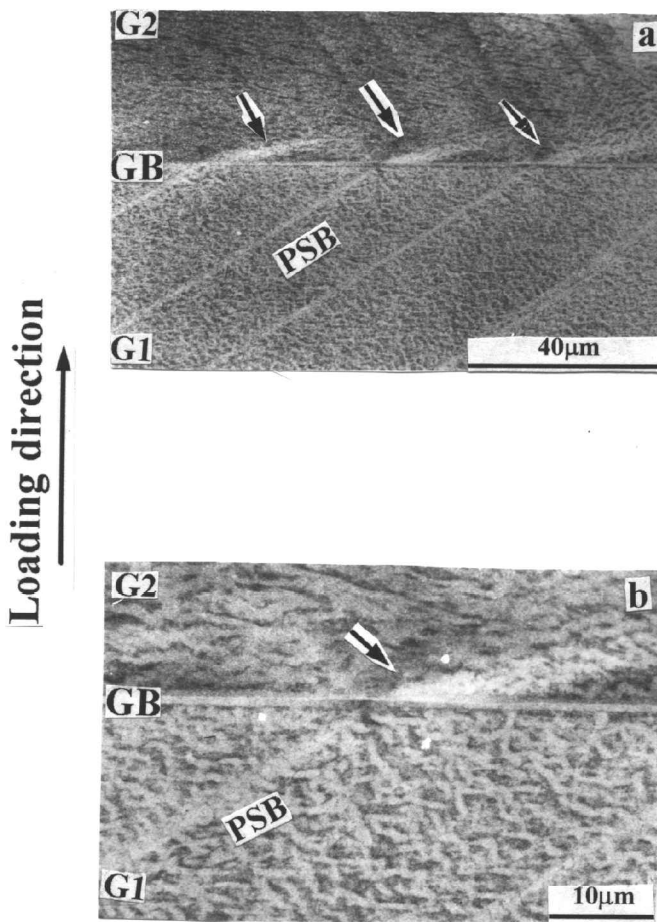
Figure 8.   The PSBs in the vicinity of the GB at $\varepsilon_{pl} = 7.6 \times 10^{-4}$ cycled for 10^4 cycles: (*a*) at a low magnification; (*b*) at a high magnification.

along a direction other than the primary slip direction in the $[\bar{5}79]$ grain. They may be the preferential sites to initiate the fatigue cracks, although the physical or mechanical essence of those affected zones needs to be further clarified.

§4. DISCUSSION

It is well known that the CSSC of the copper single crystal oriented for single slip exhibits a plateau region in the plastic shear strain range from 6×10^{-5} to 7.5×10^{-3} (Mughrabi 1978). Most investigators (Cheng and Laird 1981, Basinski and Basinski 1992) found that the plateau saturation resolved shear stress at room temperature was in the range 28–30 MPa, nearly independent of the crystal orientation inside the stereographic triangle. In the present study, it is very interesting to find that the CSSC of the $[\bar{5}\,9\,13]$-$[\bar{5}79]$ bicrystal with two single-slip-oriented grains exhibited two plateau regions, as shown in figure 3(*a*). This result has never been reported before and will be discussed as follows.

Recently, it has been noted that the plastic strains carried by two grains in a bicrystal with a perpendicular GB are different owing to the difference in orientations.

In a $[\bar{1}49]$-$[001]$ copper bicrystal with a perpendicular GB, the ratio of plastic strain in the soft grain $[\bar{1}49]$ to that in the hard grain $[001]$ in the 'steady-state' regime is approximately 5 to 1 (Peralta and Laird 1997). In the present bicrystal, as shown in figures 4 and 5, the $[\bar{5}\,9\,13]$ grain with a higher Schmid factor $(\Omega_{G1} = 0.452)$ experienced a higher resolved shear stress (see table 2) and developed a larger plastic strain than the $[\bar{5}79]$ grain with a relatively lower Schmid factor $(\Omega_{G2} = 0.406)$. In other words, the plastic strains carried by the $[\bar{5}\,9\,13]$ and $[\bar{5}79]$ grains are not equal owing to difference in their orientations.

In order to compare the cyclic saturation shear stress of copper polycrystals with that of the copper single crystals, the Taylor factor $(M = 3.06)$ or Sachs factor $(M = 2.24)$ was employed to calculate the resolved shear stress of copper polycrystals (Bhat and Lair 1978; Rasmussen and Pedersen 1980, Lukáš and Kunz 1994); Hu and Wang (1997) had attempted to compare the CSSCs between the $[\bar{1}17]$-$[\bar{3}45]$ copper bicrystal and copper polycrystals by defining an orientation factor Ω_B of the bicrystal. The mean value of the Schmid factors Ω_{G1} and Ω_{G2} of the two grains was selected:

$$\Omega_B = \frac{\Omega_{G1} + \Omega_{G2}}{2}. \tag{3}$$

They calculated the saturation resolved shear stress τ_{as} of the copper bicrystal using

$$\tau_{as} = \sigma_{as}\Omega_B = \sigma_{as}\frac{\Omega_{G1} + \Omega_{G2}}{2}. \tag{4}$$

For the bicrystal with a perpendicular GB, the axial saturation stresses σ_{as} applied on each grain are equal during cyclic deformation. However, the resolved shear stresses τ_{as}^{G1} and τ_{as}^{G2} on the primary slip direction of each grain will be different if the Schmid factors Ω_{G1} and Ω_{G2} of two grains are not equal. The saturation resolved shear stresses τ_{as}^{G1} and τ_{as}^{G2} on the primary slip direction of each grain in the bicrystal can be calculated by using equations (1) and (2). Thus, the resolved shear stress τ_{as} of the copper bicrystal calculated by using equation (4), indeed, does not represent the true resolved shear stress of any grain. As the $[\bar{5}\,9\,13]$-$[\bar{5}79]$ bicrystal became cyclically saturated, ε_{pl}^{B}, ε_{pl}^{G1} and ε_{pl}^{G2} are the axial plastic strains carried by the bicrystal, $[\bar{5}\,9\,13]$ and $[\bar{5}79]$ grains respectively and will be related as follows:

$$\varepsilon_{pl}^{B} = \varepsilon_{pl}^{G1} f_{G1} + \varepsilon_{pl}^{G2} f_{G2}, \tag{5}$$

where f_{G1} and f_{G2} are the volume fractions of the $[\bar{5}\,9\,13]$ and $[\bar{5}79]$ grains in the bicrystal. If $f_{G1} = f_{G2} = 0.5$, we have

$$2\varepsilon_{pl}^{B} = \varepsilon_{pl}^{G1} + \varepsilon_{pl}^{G2}. \tag{6}$$

As reported by Peralta and Laird (1997) and according to equations (1) and (2); the $[\bar{5}\,9\,13]$ grain with the higher Schmid factor will be subjected to a higher resolved shear stress and will carry more plastic strain than the $[\bar{5}79]$ grain with the lower Schmid factor in the $[\bar{5}\,9\,13]$-$[\bar{5}79]$ bicrystal, that is

$$\varepsilon_{pl}^{G1} > \varepsilon_{pl}^{G2}. \tag{7}$$

The above relation was supported by observations of surface slip pattern, as shown in figures 4 and 5. In combination with equations (6) and (7), the following relation between ε_{pl}^{B}, ε_{pl}^{G1} and ε_{pl}^{G2} carried by the bicrystal, $[\bar{5},9\,13]$ and $[\bar{5}79]$ grains respectively should be true, even though the exact value of ε_{pl}^{G1} and ε_{pl}^{G2} cannot been estimated easily:

$$\varepsilon_{pl}^{G2} < \varepsilon_{pl}^{B} < \varepsilon_{pl}^{G1}. \tag{8}$$

By using equations (1) and (2), the resolved shear stresses τ_{as}^{G1} and τ_{as}^{G2} of the $[\bar{5}\,9\,13]$ and $[\bar{5}79]$ grains in the bicrystal at all the applied plastic strain amplitudes have been calculated (see table 2) and are shown in figure 3 (*b*). It can be seen that the resolved shear stresses of the $[\bar{5}\,9\,13]$ and $[\bar{5}79]$ grains in the lower plateau region are 28–29 MPa and 25–26 MPa respectively. With increasing plastic strain amplitude, the resolved shear stresses of the two grains in the upper plateau region are 31–32 MPa and 28–29 MPa respectively.

From the observations and analysis above, the occurrence of two plateau regions in the CSSC of the bicrystal can be explained reasonably in terms of the results of copper monocrystals. At the beginning of cyclic deformation for the copper bicrystal, the plastic strain will be mainly carried by the $[\bar{5}\,9\,13]$ grain. With further cyclic deformation, the rapid cyclic hardening of the $[\bar{5}\,9\,13]$ grain will lead to plastic deformation in the $[\bar{5}79]$ grain. Consequently, the cyclic hardening of the $[\bar{5}\,9\,13]$ and $[\bar{5}79]$ grains will occur alternatively during initial cyclic hardening. When the copper bicrystal reaches cyclic saturation, the major portion of the plastic strain will be carried by the $[\bar{5}\,9\,13]$ grain. In connection with the surface slip patterns (see figure 4) and the dislocation structures (see figure 7) in the lower plastic strain range, it is reasonable to conclude that the lower plateau region in the CSSC of the present bicrystal is attributed to the cyclic saturation of the $[\bar{5}\,9\,13]$ grain in region B of its CSSC.

At higher plastic strain amplitudes, the plastic strain carried by the $[\bar{5}\,9\,13]$ grain will increase and reach region C in its CSSC. This conclusion is in accord with the resolved shear stress of 31–32 MPa (see table 2 and figure 3 (*b*)), the observed surface deformation bands (figure 5) and the irregular dislocation cell structures (see figure 7 (*a*)) of the $[\bar{5}\,9\,13]$ grain. In the meantime, the $[\bar{5}79]$ grain will carry more plastic strain and will saturate cyclically in region B of its CSSC. The resolved shear stress of 28–29 MPa in the $[\bar{5}79]$ grain (see table 2 and figure 3 (*b*)) and the ladder-like saturation dislocation structures (see figure 7 (*b*)) provided strong evidence for this argument.

As discussed above, the two-plateau behaviour of the CSSC in the $[\bar{5}\,9\,13]$-$[\bar{5}79]$ copper bicrystal can be reasonably explained by the following diagrammatic sketches. As shown in figure 9, the CSSC of the $[\bar{5}79]$ grain should be higher than that of the $[\bar{5}\,9\,13]$ grain owing to the difference in their orientations. In the lower plastic strain range, the cyclic saturation of the $[\bar{5}\,9\,13]$ grain in region B of its CSSC will lead to the lower plateau region. Similarly, as the plastic strain is increased, the plastic strain carried by the $[\bar{5}79]$ grain will reach region B of its CSSC. In this case, the plastic strain carried by the $[\bar{5}\,9\,13]$ grain should be in the range of region C in its
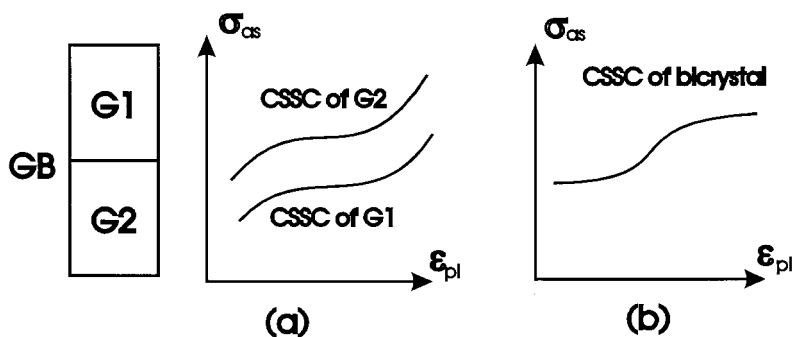

Figure 9. Illustration of the double-plateau behaviour in the present copper bicrystal.

CSSC. Consequently, the upper plateau region of the bicrystal should be attributed to the cyclic saturation of the $[\bar{5}79]$ grain in region B of its CSSC.

§5. Conclusions

Based on the cyclic deformation behaviour of a $[\bar{5}\,9\,13]$-$[\bar{5}79]$ copper bicrystal with a perpendicular GB, the following conclusions can be drawn.

(1) The CSSC of the bicrystal displayed a double-plateau region in the axial plastic strain range from 1.8×10^{-4} to 2.56×10^{-3}. The axial saturation stress in the lower plateau region is about 62–64 MPa over the plastic strain range from 1.8×10^{-4} to 1.35×10^{-3}, and the axial saturation stress in the upper plateau region is increased to about 70–71 MPa in the plastic strain range from 2.05×10^{-3} to 2.56×10^{-3}.

(2) Only the primary slip system B4 $(111)[\bar{1}01]$ was activated, in both the $[\bar{5}\,9\,13]$ and the $[\bar{5}79]$ grains and including the vicinity of the GB. The plastic strains carried by the $[\bar{5}\,9\,13]$ and $[\bar{5}79]$ grains are obvious different owing to the difference in their orientations.

(3) The cyclic saturation dislocation patterns within the $[\bar{5}\,9\,13]$ and $[\bar{5}79]$ grains and in the vicinity of the GB were observed by the SEM–ECC technique. From observations of the slip patterns and cyclic saturation dislocation patterns, it is suggested that the occurrence of the two-plateau region in the CSSC of the bicrystal resulted from the cyclic saturation of the $[\bar{5}\,9\,13]$ and $[\bar{5}79]$ grains in the region B of their CSSCs.

References

Basinski, Z. B., and Basinski, S. J. 1992, *Prog. Mater. Sci.,* **36**, 89.
Bhat, S. P., and Laird, C., 1978, *Scripta metall.,* **12**, 687.
Bretschneider, J., Holste C., and Tippelt, B., 1977, *Acta mater.,* **45**, 3755.
Cheng, A. S., and Laird, C., 1981, *Mater. Sci. Engng,* **51**, 111.
Chuang, Y. D., and Margolin, H., 1973, *Metall. Trans.* A, **4**, 1905.
Finney, J. M., and Laird, C., 1975, *Phil. Mag.,* **31**, 339.
Gong, B., Wang, Z. R., Chen, D. L., and Wang, Z. G., 1997, *Scripta Mater.,* **37**, 1605.
Hirth, J. P., 1972, *Metall. Trans.* A, **3**, 3047.
Hook, R. E., and Hirth, J. P., 1967, *Acta metall.,* **15**, 535.
Hu, Y. M., and Wang, Z. G., 1997, *Acta Mater.,* **45**, 2655.
Kocks, U. F., 1964, *Phil. Mag.,* **9**, 187.
Laird, C., Charsley, P., and Mughrabi, H., 1986, *Mater. Sci. Engng.,* **81**, 433.
Lukáš, P., and Kunz, L., 1994, *Mater. Sci. Engng.,* **33**, 207.
Peralta, P., and Laird, C., 1997, *Acta Metall.,* **45**, 3029.
Rasmussen, K. V., and Pedersen, O. B., 1980, *Acta metall.,* **28**, 1467.
Rey, C., and Zaoui, A., 1980, *Acta metall.,* **28**, 687.
Schwab, A., Bretschneider, J., Buque, C., Blochwitz, C., and Holste, C., 1996, *Phil. Mag. Lett.,* **74 ,** **449.**
Schwab, A., Meißner, O., and Holste, C., 1998, *Phil. Mag. Lett.,* **77**, 23.
Winter, A. T., 1974, *Phil. Mag.* A, **30**, 719.
Zauter, R., Petry, F., Bayerlein, M., Sommer, C., Christ, H.-J., and Mughrabi, H., 1992, *Phil. Mag.* A, **66**, 425.